ISSN: 0067-2904
GIF: 0.851

The Effect of Short Range Correlation on The Nuclear Charge Density Distribution, Elastic and Inelastic Electron Scattering Coulomb Form Factors of ^{18}O Nucleus

Adel K. Hamoudi, Abdullah S. Mdekil*
Department of Physics, College of Science, University of Baghdad, Baghdad, Iraq

Abstract

The effect of short range correlations on the inelastic longitudinal Coulomb form factors for the lowest four excited 2^+ states in ^{18}O is analyzed. This effect (which depends on the correlation parameter β) is inserted into the ground state charge density distribution through the Jastrow type correlation function. The single particle harmonic oscillator wave function is used with an oscillator size parameter b. The parameters β and b are, considered as free parameters, adjusted for each excited state separately so as to reproduce the experimental root mean square charge radius of ^{18}O. The model space of ^{18}O does not contribute to the transition charge density. As a result, the inelastic Coulomb form factor of ^{18}O comes absolutely from the core polarization transition charge density. According to the collective modes of nuclei, the core polarization transition charge density is assumed to have the form of Tassie shape. It is found that the introduction of the effect of short range correlations is necessary for obtaining a remarkable modification in the calculated inelastic longitudinal Coulomb form factors and considered as an essential for explanation the data amazingly throughout the whole range of considered momentum transfer.
PACS: 25.30.Dh; 21.60.Cs; 27.20.+n

Keywords: ^{18}O (e, e') inelastic longitudinal form factors calculated without and with the effect of short range correlations.

تاثير دالة ارتباط المدى القصير على توزيع كثافة الشحنة النووية وعوامل التشكل الكولومية للاستطارة المرنة والغير مرنة لنواة الاوكسجين -18

عادل خلف حمودي، عبدالله سوادي مديخل*
قسم الفيزياء، كلية العلوم، جامعة بغداد، بغداد ، العراق.

الخلاصة

لقد تم دراسة تاثيردالة ارتباط المدى القصير على عوامل التشكل الكولومي غير المرن. تم ادخال هذا التأثير (الذي يعتمد على معلم الارتباط β) على توزيع كثافة الشحنة للحالة الأرضية من خلال دالة الارتباط نوع Jastrow. كما تم اعتماد الدالة الموجية للمتذبذب التوافقي للجسيم المنفرد مع معلم حجم التذبذب b . في هذه الدراسة تم اعتبار β وb كمعلمات حرة تُغَير (لكل حالة متهيجة بصورة منفصلة) للحصول على النتائج العملية للجذر ألتربيعي لمعدل مربع نصف قطر الشحنة. في هذا البحث تم افتراض عدم مساهمة كثافة الشحنة الانتقالية لفضاء أنموذج الأوكسجين -18 في حسابات عوامل التشكل الكولومي غير المرن والمساهمة تكون فقط من خلال كثافة الشحنة الانتقالية لاستقطاب القلب النووي . وبموجب الانماط التجميعية للنوى، تم حساب كثافة الشحنة الانتقالية لاستقطاب القلب باستخدام Tassie shape. لقد وُجِدَ ان إدخال تأثير دالة ارتباط المدى القصير يكون ضروري للحصول على تعديل ملحوظ وتحسين النتائج النظرية لعوامل

*Email: physicsabdullah@yahoo.com

التشكل الكولومية الغير المرنة ووُجد ايضا بانها أساسية لتفسير البيانات بشكل ممتاز خلال كامل مدى للزخم المنتقل المعتمد في هذه الدراسة.

1-Introduction

Electron scattering provides more accurate information about the nuclear structure for example size and charge distribution. It provides important knowledge about the electromagnetic currents inside the nuclei. Electron scattering have been provided a good test for such evaluation since it is sensitive to the spatial dependence on the charge and current densities [1- 3].

Depending on the electron scattering, one can distinguish two types of scattering: in the first type, the nucleus is left in its ground state, that is called "elastic electron scattering" while in the second type, the nucleus is left on its different excited states, this is called "inelastic electron scattering" [4, 5]. In the studies of Massen et al. [6-8], the factor cluster expansion of Clark and co-workers [9-12] was utilized to derive an explicit form of the elastic charge form factor, truncated at the two-body term. This form, which is a sum of one- and two-body terms, depends on the harmonic oscillator parameter and the correlation parameter through a Jastrow-type correlation function [13]. This form is employed for the evaluation of the elastic charge form factors of closed shell nuclei ^{4}He, ^{16}O, ^{40}Ca and in an approximate technique (that is, for the expansion of the two-body terms in powers of the correlation parameter, only the leading terms had been kept) for the open *s - p* and *s - d* shell nuclei. Subsequently, Massen and Moustakidis [14] performed a systematic study of the effect of the SRC on *s - p* and *s – d* shell nuclei with entirely avoiding the approximation made in their earlier works outlined in [7-9] for the open shell nuclei. Explicit forms of elastic charge form factors and densities were found utilizing the factor cluster expansion of Clark and co-workers and Jastrow correlation functions which introduce the SRC. These forms depends on the single particle wave functions and not on the wave functions of the relative motion of two nucleons as was the case of our previous works [14-20] and other works [6,21,22].

It is important to point out that all the above studies were concerned with the analysis of the effect of the SRC on the elastic electron scattering charge form factors of nuclei. There has been no detailed investigation for the effect of the SRC on the inelastic electron scattering form factors of nuclei. We thus, in the present work, perform calculations with inclusion this effect on the inelastic Coulomb (longitudinal) form factors for isotopes of closed shell nuclei. As a test case, the ^{18}O isotope is considered in this study. In ^{18}O it's assumed that the Coulomb form factors of this isotope comes totally from the core polarization transition charge density. According to the collective modes of nuclei, the core polarization transition charge density (which depends on the ground state charge density distribution) is assumed to have the form of Tassie shape [23]. To study the effect of SRC (which depends on the correlation parameter β) on inelastic electron scattering charge form factors of considered nucleus, we insert this effect on the ground state charge density distribution through the Jastrow type correlation function [14]. The single particle harmonic oscillator wave function is used in the present calculations .The effect of SRC's on the inelastic Coloumb form factors for the lowest four excited 2^+ states and two excited 4^+ states in ^{18}O isotope is analyzed.

2. Theory

Inelastic electron scattering longitudinal (Coulomb) form factor involves angular momentum *J* and momentum transfer *q*, and is given by [24]

$$\left|F_J^L(q)\right|^2 = \frac{4\pi}{Z^2(2J_i+1)}\left|\left\langle f \left\| \hat{T}_J^L(q) \right\| i \right\rangle\right|^2 \left|F_{cm}(q)\right|^2 \left|F_{fs}(q)\right|^2, \quad (1)$$

where $|i\rangle = |J_i T_i\rangle$ and $|f\rangle = |J_f T_f\rangle$ are the initial and final nuclear states (described by the shell model states of spin $J_{i/f}$ and isospin $T_{i/f}$), $\hat{T}_J^L(q)$ is the longitudinal electron scattering operator, $F_{cm}(q) = e^{q^2b^2/4A}$ is the center of mass correction (which removes the spurious states arising from the motion of the center of mass when shell model wave function is used), $F_{fs}(q) = e^{-0.43q^2/4}$ is the nucleon finite size correction and assumed to be the same for protons and neutrons, A is the nuclear mass number, Z is the atomic number and b is the harmonic oscillator size parameter.

The form factor of eq.(1) is expressed via the matrix elements reduced in both angular momentum and isospin [25]

$$\left|F_J^L(q)\right|^2 = \frac{4\pi}{Z^2(2J_i+1)}\left|\sum_{T=0,1}(-1)^{T_f-T_{Z_f}}\begin{pmatrix} T_f & T & T_i \\ -T_{z_f} & 0 & T_{z_i}\end{pmatrix}\left\langle J_f T_f \left\|\hat{T}_{JT}^L(q)\right\| J_i T_i\right\rangle\right|^2 \times \left|F_{cm}(q)\right|^2 \left|F_{fs}(q)\right|^2, \tag{2}$$

where in eq. (2), the bracket ( ) is the three- J symbol, T is restricted by the following selection rule:

$$\left|T_f - T_i\right| \le T \le T_f + T_i, \tag{3}$$

and T_z is given by $T_z = \frac{Z-N}{2}$.

Where N is the neutron number

The reduced matrix elements in spin and isospin space of the longitudinal operator between the final and initial many particles states of the system including configuration mixing are given in terms of the one-body density matrix (OBDM) elements times the single particle matrix elements of the longitudinal operator [26]

$$\left\langle f \left\| \hat{T}_{JT}^L \right\| i \right\rangle = \sum_{a,b} OBDM^{JT}(i,f,J,a,b)\left\langle b \left\| \hat{T}_{JT}^L \right\| a \right\rangle, \tag{4}$$

Where a and b label single particle states (isospin included) for the shell model space. The $OBDM$ in eq. (4) is calculated in terms of the isospin-reduced matrix elements as [27]

$$OBDM(\tau_z) = (-1)^{T_f-T_Z}\begin{pmatrix} T_f & 0 & T_i \\ -T_z & 0 & T_z\end{pmatrix}\sqrt{2}\,\frac{OBDM(\Delta T=0)}{2} + \tau_z(-1)^{T_f-T_Z}\begin{pmatrix} T_f & 1 & T_i \\ -T_z & 0 & T_z\end{pmatrix}\sqrt{6}\,\frac{OBDM(\Delta T=1)}{2}, \tag{5}$$

Where τ_z is the isospin operator of the single particle.

The model space matrix elements are not adequat to describe the absolute strength of the observed gamma-ray transition probabilities, because of the polarization in nature of the core protons by the model space protons and neutrons. Therefore the many particle reduced matrix elements of the longitudinal electron scattering operator $\hat{T}_J^L(q)$ is expressed as

$$\left\langle f \left\| \hat{T}_J^L(\tau_Z,q) \right\| i \right\rangle = \left\langle f \left\| \hat{T}_J^{ms L}(\tau_Z,q) \right\| i \right\rangle + \left\langle f \left\| \hat{T}_J^{cp L}(\tau_Z,q) \right\| i \right\rangle. \tag{6}$$

The model space matrix element, in eq. (6), is given by

$$\left\langle f \left\| \hat{T}_J^{ms L}(\tau_Z,q) \right\| i \right\rangle = \int_0^\infty d\mathrm{r}\, \mathrm{r}^2\, j_J(q\mathrm{r})\, \rho_{J,\tau_Z}^{ms}(i,f,\mathrm{r}), \tag{7}$$

where $j_J(qr)$ is the spherical Bessel function and $\rho_{J,\tau_Z}^{ms}(i,f,r)$ is the model space transition charge density, expressed as the sum of the product of the $OBDM$ times the single particle matrix elements, given by [27].

$$\rho_{J,\tau_Z}^{ms}(i,f,\mathrm{r}) = \sum_{jj'(ms)}^{ms} OBDM(i,f,J,j,j',\tau_z)\left\langle j \left\| \mathrm{Y}_J \right\| j' \right\rangle R_{nl}(\mathrm{r})\, R_{n'l'}(\mathrm{r}). \tag{8}$$

Here, $R_{nl}(r)$ is the radial part of the harmonic oscillator wave function and Y_J is the spherical harmonic wave function.

The core-polarization matrix element, in eq. (6), is given by

$$\left\langle f \left\| \hat{T}_J^{cp L}(\tau_Z,q) \right\| i \right\rangle = \int_0^\infty d\mathrm{r}\, \mathrm{r}^2\, j_J(q\mathrm{r})\, \rho_{J,\tau_Z}^{cp}(i,f,\mathrm{r}), \tag{9}$$

Where $\rho^{cp}_{J\tau_z}(i,f,r)$ is the core-polarization transition charge density which depends on the model used for core polarization. To take the core-polarization effects into consideration, the model space transition charge density is added to the core-polarization transition charge density that describes the collective modes of nuclei. The total transition charge density becomes:

$$\rho_{J\tau_z}(i,f,r)=\rho^{ms}_{J\tau_z}(i,f,r)+\rho^{cp}_{J\tau_z}(i,f,r) \tag{10}$$

According to the collective modes of nuclei, the core polarization transition charge density is assumed to have the form of Tassie shape [23]

$$\rho^{cp}_{Jt_z}(i,f,r)=N_T\frac{1}{2}(1+\tau_z)\,r^{J-1}\frac{d\rho^{gs}_{ch}(i,f,r)}{dr}, \tag{11}$$

Where N_T is the proportionality constant given by [14]

$$N_T=\frac{\int_0^\infty dr\,r^{J+2}\rho^{ms}_{t_z}(i,f,r)-\sqrt{(2J_i+1)\,B(CJ)}}{(2J+1)\int_0^\infty dr\,r^{2J}\rho^{gs}_{ch}(i,f,r)}, \tag{12}$$

Which can be determind by adusting the reduced transition probability $B(CJ)$ to the experimental value, and $\rho^{gs}_{ch}(i,f,r)$ is the ground state charge density distribution of considered nuclei.

For $N=Z,$ the ground state charge densites $\rho^{gs}_{ch}(r)$ of closed shell nuclei may be related to the ground state point nucleon densities $\rho^{gs}_{p}(r)$ by[28,29]

$$\rho^{gs}_{ch}(r)=\frac{1}{2}\rho^{gs}_{p}(r), \tag{13}$$

in unit of electronic charge per unit volume (e.fm^{-3}).

An expression of the correlated density $\rho^{gs}_{p}(r)$ (where the effect of the SRC's is included), consists of one- and two-body terms, is given by [30]

$$\begin{aligned}\rho^{gs}_{p}(r)&\approx N_D\left[\left\langle\hat{O}_r\right\rangle_1+\left\langle\hat{O}_r\right\rangle_2\right]\\&\approx N_D\left[\left\langle\hat{O}_r\right\rangle_1-2O_{22}(r,\beta)+O_{22}(r,2\beta)\right],\end{aligned} \tag{14}$$

Where N_D is the normalization factor and $\hat{O}_r$ is the one body density operator given by

$$\hat{O}_r=\sum_{i=1}^{A}\hat{o}_r(i)=\sum_{i=1}^{A}\delta(\vec{r}-\vec{r}_i). \tag{15}$$

The correlated density $\rho^{gs}_{p}(r)$ of eq. (14), which is truncated at the two-body term and originated by the factor cluster expansion of Clark and co-workers [9-11], depends on the correlation parameter β through the Jastrow-type correlation

$$f(r_{ij})=1-\exp[-\beta(\vec{r}_i-\vec{r}_j)^2], \tag{16}$$

Where $f(r_{ij})$ is a state-independent correlation function, which has the following properties: $f(r_{ij})\to 1$ for large values of $\vec{r}_{ij}=\left|\vec{r}_i-\vec{r}_j\right|$ and $f(r_{ij})\to 0$ for $\vec{r}_{ij}\to 0.$ It is so clear that the effect of SRC's, inserted by the function $f(r_{ij}),$ becomes large for small values of SRC parameter β and vice versa.The one-body term, in eq. (14), is well known and given by

$$\begin{aligned}\left\langle\hat{O}_r\right\rangle_1&=\sum_{i=1}^{A}\left\langle i\left|\hat{o}_r(1)\right|i\right\rangle\\&=4\sum_{nl}\eta_{nl}(2l+1)\frac{1}{4\pi}\phi^*_{nl}(r)\phi_{nl}(r),\end{aligned} \tag{17}$$

Where η_{nl} is the occupation probability of the state nl and $\phi_{nl}(r)$ is the radial part of the single particle harmonic oscillator wave function.
The two-body term, in eq. (14), is given by [30]

$$O_{22}(r,z) = 2\sum_{i<j}^{A} \left\langle ij \left| \hat{o}_r(1) g(r_1, r_2, z) \right| ij \right\rangle_a, \qquad (z = \beta,\ 2\beta) \tag{18}$$

Where

$$g(r_1, r_2, z) = \exp(-zr_1^2) \exp(-zr_2^2) \exp(2zr_1 r_2 \cos w_{12}), \tag{19}$$

The form of the two-body term $O_{22}(r,z)$ is then originated by expanding the factor $\exp(2zr_1 r_2 \cos w_{12})$ in the spherical harmonics and expressed as [30]

$$\begin{aligned} O_{22}(r,z) &= 4 \sum_{n_i l_i, n_j l_j} \eta_{n_i l_i} \eta_{n_j l_j} (2l_i + 1)(2l_j + 1) \\ &\times \left\{ 4A_{n_i l_i n_j l_j}^{n_j l_j n_i l_i 0}(r,z) - \sum_{k=0}^{l_i + l_j} \left\langle l_i 0 l_j 0 \middle| k0 \right\rangle^2 A_{n_i l_i n_j l_j}^{n_j l_j n_i l_i k}(r,z) \right\}, \qquad (z = \beta,\ 2\beta) \end{aligned} \tag{20}$$

Where

$$\begin{aligned} A_{n_1 l_1 n_2 l_2}^{n_3 l_3 n_4 l_4 k}(r,z) &= \frac{1}{4\pi} \phi_{n_1 l_1}^*(r) \phi_{n_3 l_3}(r) \exp(-zr^2) \\ &\times \int_0^\infty \phi_{n_2 l_2}^*(r_2) \phi_{n_4 l_4}(r_2) \exp(-zr_2^2)\ i_k(2zrr_2) r_2^2 dr_2 \end{aligned} \tag{21}$$

and $\left\langle l_i 0 l_j 0 \middle| k0 \right\rangle$ is the Clebsch-Gordan coefficients.

It is important to point out that the expressions of eqs. (17) and (20) are originated for closed shell nuclei with $N = Z,$ where the occupation probability η_{nl} is 0 or 1. To extend the calculations for isotopes of closed shell nuclei, the correlated charge densities of these isotopes are characterized by the same expressions of eqs. (17) and (20) (this is because all isotopic chain nuclei have the same atomic number Z) but this time different values for the parameters b and β are utilized.
The mean square charge radii of nuclei are defined by

$$\left\langle r^2 \right\rangle = \frac{4\pi}{Z} \int_0^\infty \rho_{ch}^{gs}(r)\, r^4 dr, \tag{22}$$

Where the normalzation of the charge density distribution $\rho_{ch}^{gs}(r)$ is given by

$$Z = 4\pi \int_0^\infty \rho_{ch}^{gs}(r)\, r^2 dr \tag{23}$$

The elastic electron scattering form factor from spin zero nuclei can be determined by the ground-state charge density distributions (CDD). In the plane wave born approximation (PWBA), the incident and scattered electron waves are considered as plane waves, and the CDD is real and spherically symmetric, therefore the form factor is simply the Fourier transform of the CDD, i.e.

$$F(q) = \frac{4\pi}{Z} \int_0^\infty \rho_0(r)\, j_0(qr) r^2 dr, \tag{24}$$

Where $\rho_0(r)$ is the ground state CDD of considered nuclei. Introducing the center of mass and nucleon finite size corrections into eq. (24), we get

$$F(q) = \frac{4\pi}{Z} \int_0^\infty \rho_0(r)\, j_0(qr) r^2 dr\, F_{cm}(q) F_{fs}(q) \tag{25}$$

In the limit of $q \to 0,$ the target nucleus will be considered as a point particle and with the help of the normalization condition of eq. (23), the form factor is equal to unity, i.e., $F(q = 0) = 1.$

To study the effect of SRC's on the elastic longitudinal charge form factors, the correlated charge density of eq. (13) will be used in eq. (25), i.e., $\rho_0(r) = \rho_{ch}^{gs}(r)$.

3.Results and Discussion

The effect of the SRC on the ground state CDD, elastic electron scattering charge form factors and inelastic Coulomb (longitudinal) C2 form factors for ^{18}O nucleus is studied. The CDD (based on using the single particle harmonic oscillator wave functions with oscilator size parameter b and occupation probabilities $\eta_{1s} = 1$ and $\eta_{1p} = 1)$ is calculated by eq.(13) together with eqs. (14), (17) and (20). The calculated CDD without the effect of the SRC (i.e., when the correlation parameter $\beta = 0)$ is obtained by adjusting the oscillator size parameter b so as to reproduce the experimental root mean square (rms) charge radius ($< r^2 >_{\exp}^{1/2} = 2.727 \pm 0.02$ fm) of ^{18}O. While the calculated CDD with the effect of the SRC (i.e., when $\beta \neq 0)$ is obtained by adjusting both parameters b and β so as to reproduce the experimental rms charge radius of ^{18}O. The elastic electron scattering charge form factors which is simply the Fourier transform of the CDD is calculated by eq. (25). The dependence of the CDD (in fm^{-3}) on r (in fm) for ^{18}O is displayed in Figures-1 to -3.

In Figure-1, we explore the effect of the oscillator size parameter on the CDD and on the elastic charge form factors of ^{18}O. Here, the correlation parameter is fixed with a value of $\beta = 0$ while the oscillator size parameter is taken with different values, such as $b = 1.6$ fm (the dashed curves), $b = 1.7$ fm (the long-dashed curves) and $b = 1.8$ fm (the solid curves). Figure-1(a) shows that the increasing of the parameter b leads to reduce notably the central part ($r \leq 2.5$ fm) of the CDD and shift slightly the tail part ($r > 2.5$ fm) of the CDD toward the higher values of r. This means that the probability of moving the charged protons from the central region toward the surface of the nucleus will increase with enlarging the values of the oscillator size parameter b. Figure-1(b) exhibits that the increasing of the values of b leads to shift clearly the diffraction minimum to the lower values of momentum transfer q.

In Figure-2, we repeat the calculations as in Figure-1 but this time the oscillator size parameter is fixed with a value of $b = 1.8$ fm whereas the correlation parameter is taken with different values such as, $\beta = 2$ fm^{-2} (the dashed curves), $\beta = 2.5$ fm^{-2} (the long-dashed curves) and $\beta = 3$ fm^{-2} (the solid curves). Figure-2(a) demonstrates that the increasing of the values of the correlation parameter β leads to increase significantly the central region of the CDD and vice versa. Figure-2(b) shows that the increasing of the values of β leads to shift slightly the diffraction minimum to the higher values of momentum transfer q as well as reduce slightly the enhancement in the first maximum and vice versa. Inspection to the Figures-1 and -2 immediately provides the conclusion that the parameters b and β have an opposite effect on the both calculations of the CDD and elastic charge form factors.

In Figure-3, we compare the calculated CDD [Figure-3(a)] and elastic charge form factors [Figure-3(b)] of ^{18}O with those of experimental data (the open circles). The dashed curves are the calculated results without the inclusion of the effect of the SRC obtained with $\beta = 0$ and $b = 1.82$ fm. The solid curves are the calculated results with including the effect of the SRC obtained with $\beta = 3.18$ fm^{-2} and $b = 1.79$ fm. Figure-3(a) illustrates that the calculated CDD of the dashed curve (without the effect of the SRC) and the solid curve (with the effect of the SRC) are not in such a good agreement with those of the experimental data, especially in the central region ($r \leq 2$ fm) of the distributions. Figure-3(b) demonstrates that the calculated elastic charge form factors of the dashed and solid curves are in good agreement with those of experimental data. Moreover, inspection to the Figure-3(b) gives an indication that the solid curve is better describing the experimental data than that of the dashed curve, particularly in the region of momentum transfer $q \geq 1.5$ fm.

The SRC effect on the inelastic Coulomb (longitudinal) C2 form factors for the lowest four states of $J^{\pi} = 2^{+}, T = 1$ in ^{18}O are also studied. The Coulomb form factor in ^{18}O comes totally from the core-polarization transition charge density because the two active neutrons, which move in the model

space of this nucleus, give no contribution [i.e., $\rho^{ms}_{J,\tau_Z}(i,f,r)=0$] .The SRC effect is introduced into the ground state charge density distribution through the Jastrow type correlation function. According to the collective modes of nuclei, the core polarization transition charge density is evaluated by adopting the Tassie model [eq. (11)], where this model depends on the ground state charge density distribution. The proportionality constant N_T [eq. (12)] is estimated by adjusting the reduced transition probability $B(CJ)$ to the experimental value. The CDD calculated without the effect of the SRC depends only on one free parameter (namely the parameter b), where b is fixed with a value of $b=1.82$ fm so as to reproduce the experimental rms charge radius of ^{18}O. While the CDD calculated with the effect of the SRC depends on two free parameters (namely the harmonic oscillator size parameter b and the correlation parameter β), where these parameters are chosen for each excited state separately so as to reproduce the experimental rms charge radius of ^{18}O.

In Table-1, we display the experimental excitation energies E_x (MeV), experimental reduced transition probabilities $B(CL;0^+_1\rightarrow L^+)$ (e^2 fm^{2L}) and the chosen values for the parameters b and β for each excited state.The root mean square (rms) charge radius calculated with the effect of the SRC is also displayed in this table and compared with that of experimental result. It is evident from this table that the values of the parameter b employed for calculations with the effect of the SRC are smaller than those of without the SRC ($b=1.82$ fm). This is attributed to the fact that the introduction of the SRC leads to enlarge the relative distance of the nucleons (i.e., to enlarge the size of the nucleus) whereas the parameter b (which is proportional to the radius of the nucleus) should become smaller so as to reproduce the experimental rms charge radius of the considered nucleus.

The inelastic Coulomb $C2$ form factors for different transitions ($J^\pi_{gs}T_{gs}\rightarrow J^\pi_f T_f$) in ^{18}O are displayed in Figures-4-7. It is obvious that all transitions considered in these figures are of an isovector character. Besides, the parity of them does not change. Here, the calculated inelastic $C2$ form factors are plotted versus the momentum transfer q and compared with those of experimental data. The dashed and solid curves are the calculated inelastic Coloumb $C2$ form factors without and with the inclusion of the effect of SRC's, respectively. The open circles and open squares are those of experimental data taken from [33] and [34]. In Figure-4, we display the inelastic Coulomb $C2$ form factors for the transition $0^+_1 1\rightarrow 2^+_1 1$ ($E_x=1.982$ MeV and $B(C2)=44.8\pm1.3$ e^2.fm^4 [33]). The calculated $C2$ form factors with the effect of SRC's are obtained using the values of $b=1.77$ fm and $\beta=3.18$ fm^{-2}. Here, both the dashed curve (without the effect of the SRC) and the solid curve (with the effect of the SRC) predict clearly the experimental data (the open circle symbols) [33] throughout the whole range of momentum transfer q, where both the behavior and the magnitude of these calculated curves are in very good agreement with those of experimental data. This figure shows that the inclusion of the effect of the SRC leads to enhance the calculated $C2$ form factors (the solid curve), especially at the region of momentum transfer $2<q<2.7$ fm^{-1}, and consequently leads to improve the degree of agreement with those of experimental data. It is clear that the magnitude of the experimental $C2$ form factors along the first and second maxima as well as along the diffraction minimum are very well reproduced by the solid curve. The rms charge radius calculated with the above values of b and β is 2.711 fm, which is in good agreement with the experimental value.

In Figure-5, we demonstrate the inelastic Coulomb $C2$ form factors for the transition $0^+_1 1\rightarrow 2^+_2 1$ ($E_x=3.919$ MeV and $B(C2)=22.2\pm1.0$ e^2.fm^4 [33]). The calculated $C2$ form factors (the solid curve) are obtained via utilizing the values of $b=1.78$ fm and $\beta=1.405$ fm^{-2}. It is apparent from this figure that the calculated form factors without the effect of the SRC (the dashed curve) are unsuccessful for describing the experimental data (the open circle symbols) [33]. Incorporating the effect of the SRC leads to give a remarkable improvement in the calculated form factors (the solid curve) and then leads to describe the data astonishingly for all range of momentum transfer. It is clear that the magnitude of the experimental form factors along the diffraction minimum as well as along

the first and second maxima is fine reproduced by the solid curve. The rms charge radius evaluated by utilizing the above values of b and β is 2.901 fm, which is larger than the experimental value by 0.174 fm, which corresponds to an increase of approximately 6.37 % of the experimental value.

In Figure-6, we present the inelastic Coulomb $C2$ form factors for the transition $0_1^+1 \rightarrow 2_3^+1$ ($E_x = 5.250$ MeV and $B(C2) = 28.3 \pm 1.5\ e^2.\text{fm}^4$ [34]). The calculated $C2$ form factors (the solid curve) are obtained by employing the values of $b = 1.80$ fm and $\beta = 2.15$ fm^{-2}. This figure illustrates that the calculated result displayed by the dashed curve (without the effect of the SRC) does not predict correctly the experimental data, where the diffraction minimum of this curve is not reproduced in the correct place of momentum transfer as well as the experimental data are over predicted for the first maximum and under predicted for the second maximum. Introducing the effect of the SRC leads to provide a notable modification in the calculated $C2$ form factors displayed by the solid curve and subsequently predicts the data amazingly throughout the whole range of considered momentum transfer. The rms charge radius estimated by using the above values of b and β is 2.802 fm, which is bigger than the experimental value by 0.075 fm, which corresponds to an increase of about 2.75 % of the experimental value. In Figure-7, we exhibit the inelastic Coulomb $C2$ form factors for the transition $0_1^+1 \rightarrow 2_4^+1$ ($E_x = 8.210$ MeV and $B(C2) = 7.3 \pm 4.2\ e^2.\text{fm}^4$ [33]). The calculated inelastic $C2$ form factors revealed by the solid curve (with the effect of the SRC) are obtained with applying the values of $b = 1.73$ fm and $\beta = 2.98$ fm^{-2}. This figure shows that the shape and the magnitude of the $C2$ form factors exhibited by the dashed curve (without the effect of SRC's) explain the data reasonably for all range of considered momentum transfer, where the locations of the first diffraction maximum and minimum are very well reproduced by this curve. Taking into account the effect of the SRC leads to enhance slightly the calculated form factors as seen by the solid curve. Accordingly, the $C2$ form factors exhibited by the solid curve are in general closer to the experimental data, especially at the region of $q \geq 1.5$ fm^{-1}. The rms charge radius calculated by applying the above values of b and β is 2.660 fm, which is less than the experimental value by 0.067 fm, which corresponds to a decrease of nearly 2.45 % of the experimental value.

4. Conclusions

The effect of the SRC on the CDD, elastic electron scattering form factors and inelastic Coulomb $C2$ form factors for the lowest four excited 2^+ states is analyzed. This effect is included in the present calculations through the Jastrow type correlation function. As the model space of ^{18}O does not contribute to the transition charge density, the inelastic Coulomb form factor of ^{18}O comes completely from the core polarization transition charge density. According to the collective modes of nuclei, the core polarization transition charge density is assumed to have the form of Tassie shape. It is concluded that the introduction of the effect of the SRC is necessary for obtaining a notable modification in the calculated elastic and inelastic Coulomb form factors and also essential for explanation the data astonishingly throughout the whole range of considered momentum transfer.

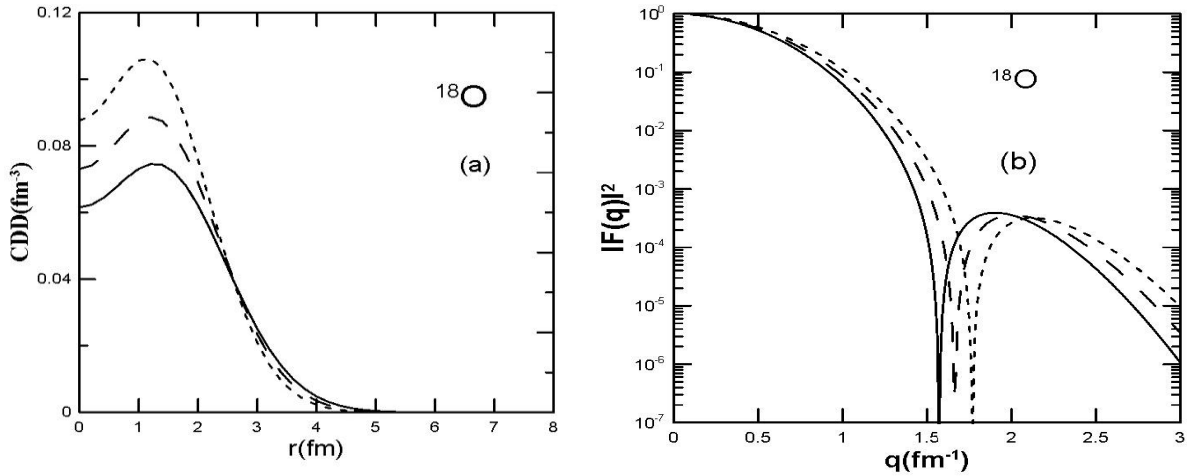

Figure 1- The effect of the oscillator size parameter on the CDD [Figure-1 (a)] and on elastic charge form factors [Figure-1 (b)] of ^{18}O. The calculated results correspond to the values for the parameters $\beta = 0,\ b = 1.6$ (the dashed curve), $\beta = 0,\ b = 1.7$ (the long-dashed curve) and $\beta = 0,\ b = 1.8$ (the solid curve).

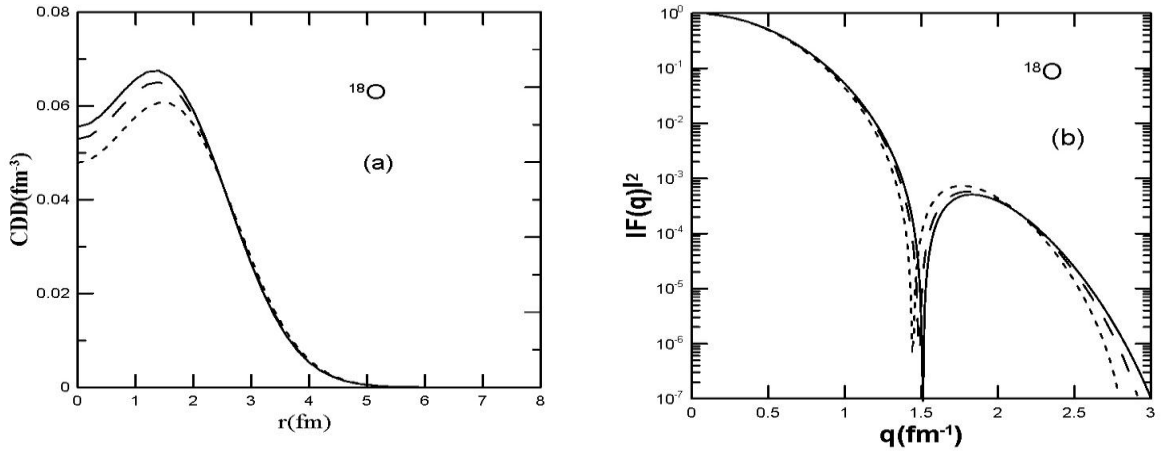

Figure 2-The effect of the correlation parameter on the CDD [Figure-2 (a)] and on elastic charge form factors [Figure-2 (b)] of ^{18}O. The calculated results correspond to the values for the parameters $\beta = 2,\ b = 1.8$ (the dashed curve), $\beta = 2.5,\ b = 1.8$ (the long-dashed curve) and $\beta = 3,\ b = 1.8$ (the solid curve).

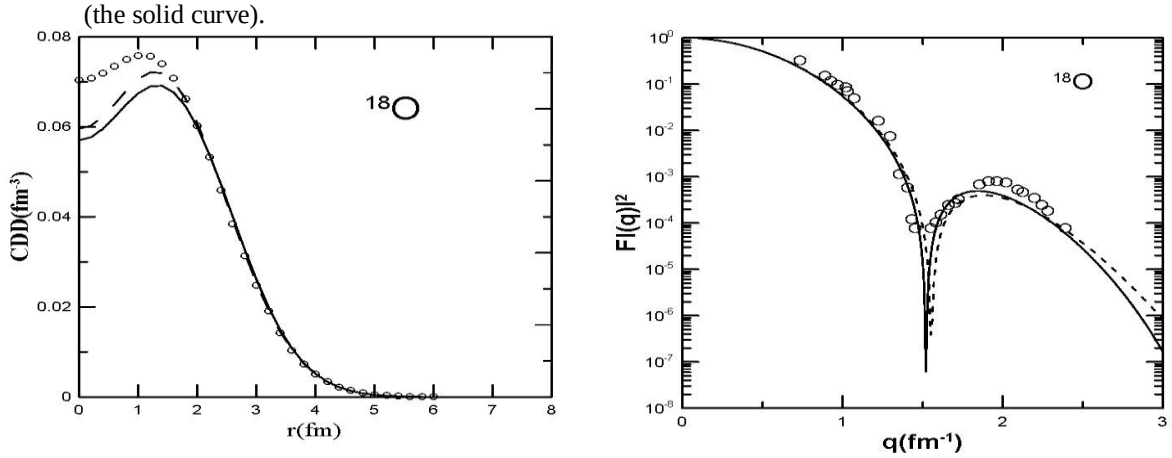

Figure 3- The calculated CDD and elastic charge form factors are compared with those of experimental data. The dashed curve corresponds to the values for the parameters $\beta = 0$ and $b = 1.82$ fm, the solid curve corresponds to the values for the parameters $\beta = 3.18$ fm^{-2} and $b = 1.79$ fm while the open circles in Figure-3(a) and 3(b) are the experimental data taken from [31] and [32], respectively.

Table 1- The experimental excitation energies and reduced transition probabilities, the chosen values for the parameters b and β as well as the root mean square (rms) charge radius calculated with the effect of the SRC of ^{18}O.

State	*Ex* (MeV)	$B(CL)$ (e^2 fm^{2L})	b (fm)	β (fm^{-2})	$< r^2 >_{cal.}^{1/2}$ (fm)	$< r^2 >_{\exp.}^{1/2}$ (fm)
2_1^+	1.982 [33]	44.8 ± 1.3 [33]	1.77	3.180	2.711	2.727 (20) [30]
2_2^+	3.919 [33]	22.2 ± 1.0 [33]	1.78	1.405	2.901	
2_3^+	5.250 [33]	28.3 ± 1.5 [33]	1.80	2.150	2.802	
2_4^+	8.210 [34]	7.3 ± 4.2 [34]	1.73	2.980	2.660	

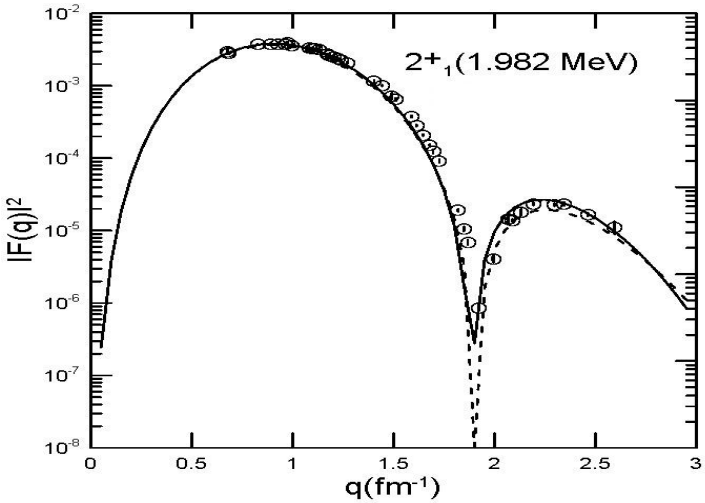

Figure 4- Inelastic Coulomb $C2$ form factors for the transition to the 2_1^+1 (1.982 MeV) state. The long-dashed and solid curves are the calculated $C2$ form factors without and with the inclusion of the effect of the SRC, respectively. The open circle symbols are those of the experimental data taken from ref. [33].

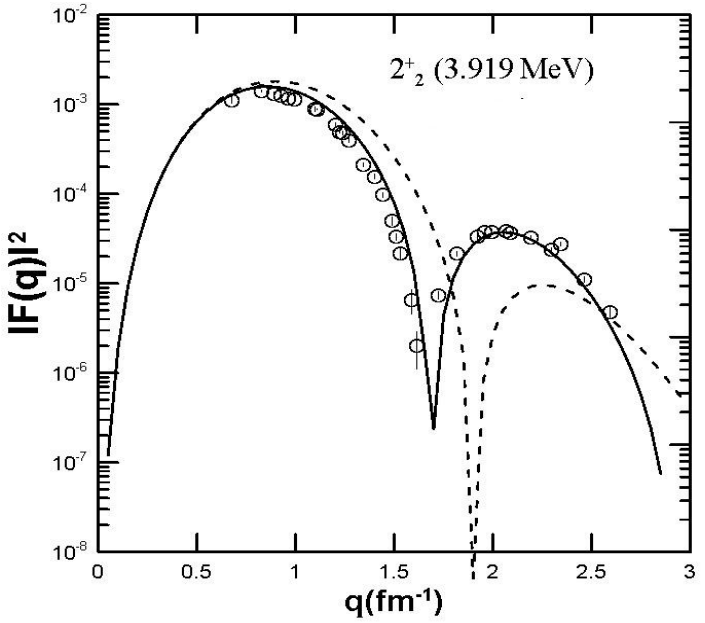

Figure 5- Inelastic Coulomb $C2$ form factors for the transition to the 2_2^+1 (3.919 MeV) state. The dashed and solid curves are the calculated $C2$ form factors without and with the inclusion of the effect of the SRC, respectively. The open circle symbols are those of the experimental data taken from ref. [33].

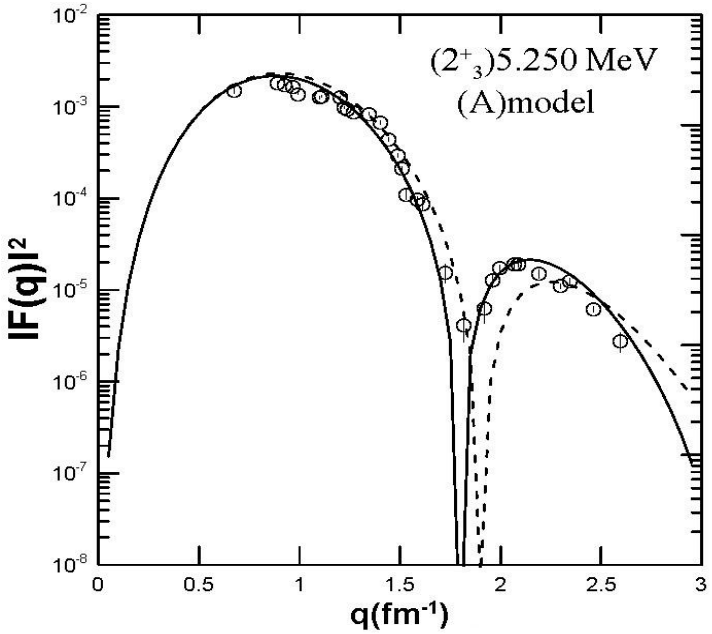

Figure 6- Inelastic longitudinal $C2$ form factors for the transition to the $2^+_3 1$ (5.250 MeV) state. The dashed and solid curves are the calculated $C2$ form factors without and with the inclusion of the effect of the SRC, respectively. The open circle symbols are the experimental data taken from ref. [33].

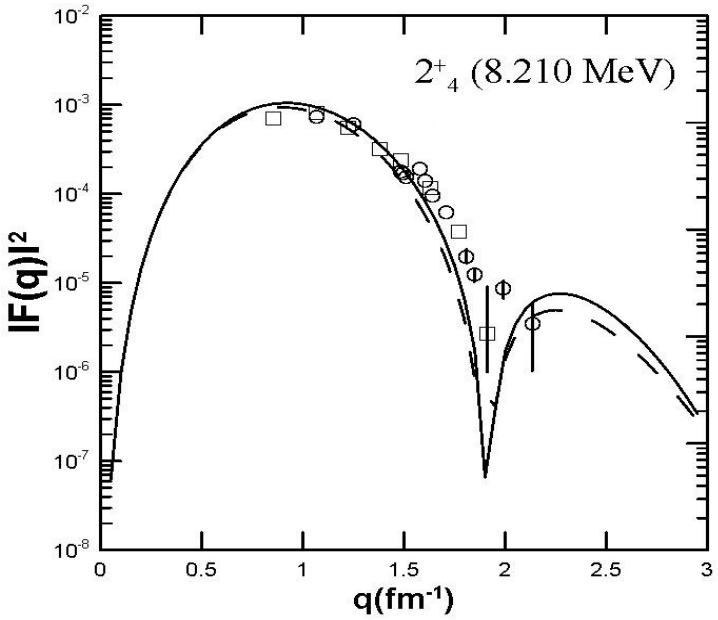

Figure 7- The inelastic longitudinal $C2$ form factors for transition to the $2^+_4 1$ (5.250 MeV) state. The dashed and solid curves are the calculated $C2$ form factors without and with the inclusion of the effect of the SRC, respectively. The open square and open circle symbols are the experimental data taken from ref. [34].

References

1. Dubach, J. Koch, J.H. and Donnelly,T.W. **1976**. Exchange currents in electron scattering from light nuclei. , *Nuclear Physics*, A271, 279-316.
2. Sato,T. Odagawa,N. Ohtsubo, H. and Lee ,T.S. **1994**. Nuclear structure studies with (e, e'), (π, π'), and (γ, π) reactions: Applications to ^{10}B, *Physical Review*, C49(2), pp: 776-788.
3. Bergstrom,J.C. Kowalski, S.B. and Neuhausen,R. **1982**. Elastic magnetic form factor of ^{6}Li, *Physical Review*, C25(3), 1156-1167.
4. Uberall,H. **1971**. *Electron Scattering From Complex Nuclei*. Part B, Academic Press, New York.

5. Millener,D.J. Sober,D. I. Crannel,H. O'Brien,J. T. Fagg,L. W. Kowalski,S. Williamson, C. F. and Lapikas. **1989**. Inelastic electron scattering from ^{13}C. *Physical Review*, C39 (1), pp: 14-39.

6. Massen,S.E. Nassena, H.P. and Panos,C.P. **1988**. A formula for the charge form factor of closed-shell nuclei and its application to ^{16}O. *Journal of Phyics*, G 14(6), 753.

7. Massen, S.E. and Panos,C.P. **1989**. An approximate treatment of the correlated charge form factor of light nuclei, *Journal of Phyics*, G 15, pp: 311-319.

8. Massen, S.E. **1990**. Correlated charge form factor and densities of the s-d shell nuclei. *Journal of Phyics*, G 16 (3), 1713.

9. Clark, J.W. and Ristig,M.L. Cluster-expansion procedures for the correlated charge form factor. **1970**. *Nuovo Cimento*, A 70, pp: 313-322.

10. Ristig,M.L. Ter Low, W.J. and Clark, J.W. **1971**.Tensor Correlations in Nuclear Matter, *Physical Review* ,C 3(4), pp: 1504-1513.

11. Clark,J.W. **1979**. Variational theory of nuclear matter, *Progress in Particle and Nuclear Physics*, 2, pp: 89-199.

12. Jastrow,R. **1955**. Many-body problem with strong forces. *Physical Review*, 98, pp: 1479-1484.

13. Massen, S.E. and Moustakidis, Ch. C**.1999**. Systematic study of the effect of short range correlations on the form factors and densities of s-p and s-d shell nuclei, *Physical Review*, C 60, 24005.

14. Sharrad, F.I. **2007**. The effect of two- body short range correlation functions on the charge density distributions and form factors of some light nuclei, Ph.D. Thesis. Department of Physics, College of Science, University of Baghdad, Baghdad, Iraq.

15. Flaiyh, Gaith Naima **2008**. The effect of two- body correlation functions on the density distributions and electron scattering form factors of some light nuclei, Ph.D. Thesis. Department of Physics, College of Science, University of Baghdad, Baghdad, Iraq.

16. Hamoudi, A. K. Radhi, R. A. Flaiyh, G. N. and Shrrad,F. I. **2010**.The effect of two body correlations on the charge density distributions and elastic electron scattering form factors for some 2s-1d shell nuclei, *Journal of Al-Nahrain University-Science*, 13(4) , pp. 88-98.

17. Hamoudi,A. K. Radhi, R. A. and Flaiyh,G. N. **2010**. Core Polarization Effects on the Inelastic Longitudinal C2 Form Factors of Open sd-Shell Nuclei, *Engineering & Technology Journal*, 28(19), pp: 5869-5880.

18. Hamoudi,A. K. Radhi, R. A. and Flaiyh,G. N. **2011**. Calculation of the longitudinal electron scattering form factors for the 2s-1d shell nuclei. *Iraqi Journal of Physics*, 9(14), pp.51-66.

19. Sharrad,F. I. Hamoudi, A. K. Radhi,R. A. Abdullah,Hewa Y. Okhunov, A. A. and Kassim,H. Abu. **2013**. Elastic electron scattering from some light nuclei, *Chinese Journal of physics*, 51(3), pp: 452-465.

20. Sharrad,F. I. Hamoudi,A. K. Radhi,R. A. and Abdullah, H. Y. **2013**. Inelastic electron scattering from light nuclei, *Journal of the National Science Foundation of Sri Lanka*, 41(3), pp.209-217.

21. Atti,Ciofi degli .**1969**.Elastic scattering of high-energy electrons and correlation structure of light nuclei, *Nuclear Physics*, A 129, pp:350-368.

22. Nassena,H.P. **1981**. The factor cluster expansion model operator approach and the charge form factor of the ^{4}He nucleus, *Journal of Phyics*, G14, pp: 927-936.

23. Tassie ,L.J. **1956**. Model of nuclear shape oscillations for γ- transitions and electron excitation, *Australian Journal of physics*, 9,407.

24. Brown,B.A. Wildenthal,B.H. Williamson, C.F. Rad,F.N. Kowalski,S. Crannell Hall and O'Brien,J.T. **1985**. Shell-model analysis of high-resolution data for elastic and inelastic electron scattering on ^{19}F, *Physical Review*, C 32(4) , pp: 1127-1156.

25. Donnelly, T.W. and Sick,I. **1984**. Elastic magnetic electron scattering from nuclei, *Reviews of Modern Physics*, 56 (3), pp: 461-566.

26. Brussard, P.J. and Glaudemans,P.W.M. **1977**. *Shell-model applications in nuclear spectroscopy*, North Holland, Amsterdam.

27. Brown, B. A. Radhi, A.R. and Wildenthal,B.H. **1983**. Electric quadrupole and hexadrupole nuclear excitations from the perspectives of electron scattering and modern shell-model theory, *Physics Reports*, 101(5), pp: 313-358.

28. Hamoudi,A.K. Hasan, M.A. and Ridha,A.R. **2012**.Nucleon momentum distributions and elastic electron scattering form factors for som 1p-shell nuclei.*Pramana Journal of physics*,78(5), pp: 737- 748.

29. Ridha,A. R. **2006**. Nucleon Momentum Distributions in Closed and Open Shell Nuclei, M.Sc. Thesis. Department of Physics, College of Science, University of Baghdad, Baghdad, Iraq.

30. Massen,S.E. and Moustakidis,Ch. C. **1999**. Systematic study of the effect of short range correlations on the form factors and densities of s-p and s-d shell nuclei, *Physical Review*, C 60, 24005.

31. De Vries, H. De Jager, C.W. and De Vries, C. **1987**. Nuclear charge-density-distribution parameters from elastic electron scattering. *Atomic data and nuclear data tables*, 36, 495-536.

32. Kuchta,R. **1988**.Microscopic boson description of proton-neutron systems: Application to elastic and inelastic electron scattering from ^{18}O and ^{20}Ne, *Physical Review*, C38 (3), 1460-1474.

33. Norum,B.E. Hynes, M.V. Miska, H. Bertozzi,W. Kelly,J. Kowalski,S. . Rad, F. N. Sargent,C.P. Sasanuma,T. Turchinetz,W. **1982**. Inelastic electron scattering from ^{18}O, *Physical Review*, C 25 (4), 1778-1800.

34. Manlly,D.M. Millener,D.J. Berman,B.L. Bertozzi,W. Buti,T.N. Finn,J.M. Hersma,F.W. Hyde-Wright,C.E. Hynes,M.V. Kelly,J.J. Kovash, M.A. Kowalski,S. Louri, R.W. Murdock,M. Norum, B.E. Pugh, and B. Sargent,C.P. **1990**. Electroexcitation of rotational bands in ^{18}O, *Physical Review*, C 41(2), 448-457.